Synthetic proper elements for outer main belt asteroids

Z. KNEŽEVIĆ[1] and A. MILANI[2]
[1] Astronomical Observatory, Volgina 7, 11160 Belgrade 74, Yugoslavia, e-mail: zoran@aob.bg.ac.yu
[2] Department of Mathematics, Via Buonarroti 2, 56127 Pisa Italy, e-mail: milani@dm.unipi.it

May 31, 2000

Abstract

For the orbits with low to moderate inclination and eccentricity, in the asteroid main belt, the analytically computed proper elements are accurate to a level very close to the best result achievable by any analytical theory. This fundamental limitation results from the infinite web of resonances and because of the occurrence of chaotic motions. Still, there are some regions of the belt in which these proper elements are of degraded accuracy, thus preventing a reliable definition of asteroid families and detailed studies of the dynamical structure. We have used a different method to compute asteroid proper elements, following the approach introduced in the LONGSTOP project to describe the secular dynamics of the major outer planets. By applying purely numerical techniques, we produced so-called "synthetic" proper elements for a catalog of $10,256$ asteroids with osculating semimajor axes between 2.5 and 4.0 AU.

The procedure consisted of simultaneous integration of asteroid and planetary orbits for 2 Myr, with online filtering of the short-periodic perturbations. The output of the integration was spectrally resolved, and the principal harmonics (proper values) extracted from the time series. For each asteroid we have also tested the accuracy and stability in time of the proper elements, and estimated the maximum

Lyapounov Characteristic Exponent to monitor the chaotic behaviors. This provided information on the reliability of the data for each orbit, in particular allowing to select $1,852$ cases for an extended integration (10 Myr) of the orbits showing instability. The results indicate that for more than half of the cases the proper elements have a time stability improved by more than a factor 3 with respect to the elements computed by the previous analytical theory. But of course there are also unstable cases for which the proper elements are less accurate and reliable, the extreme examples being 23 orbits exibiting hyperbolic escape from the solar system. This form of escape from the asteroid belt could be responsible for a significant mass loss over the age of the solar system.

Keywords: asteroids, proper elements, chaos, families.

1 Introduction

The main motivation to produce "yet another set of asteroid proper elements" is that for many asteroids the currently available proper elements, derived by means of an analytical theory by Milani and Knežević ([1990, 1992, 1994]), are not (any more) accurate enough, at least when these elements are used to identify and study asteroid dynamical families, and to try to understand the dynamical structure of the asteroid belt.

In the densely populated low to moderate eccentricity and inclination region of the asteroid main belt, the proper elements computed analytically are accurate to a level very close to the best result achievable by any analytical theory (Milani and Knežević [1994]). This because there is an infinite web of resonances (Arnold [1963]), and because of the occurrence of chaotic motions. It is not yet clear whether the asteroid belt is a big chaotic sea (although with diffusion times on the order of billions of years), or it is structured in the sense described by Nekoroshev theorem for quasi-integrable Hamiltonian systems (Morbidelli and Guzzo [1997]). However, it is now established that the motions of asteroids are basically chaotic, and that only the dynamical mechanisms responsible for this chaos, the time scales involved, and the size and form of the resulting macroscopic instabilities are different (Milani et al. [1997]). Moreover, asteroids are not allowed to be less chaotic than the perturbing major planets (Laskar [1989], Nobili et al. [1989]), and this "induced chaos" introduces a chaotic noise in the asteroid proper elements of the order of 10^{-4} (Milani and Knežević [1994]).

The typical instability of the current analytical proper elements in proper e and $sinI$ is $\leq$ 0.0015 over 5 Myr (Milani and Knežević [1994]). This accuracy was enough for Zappalà et al. ([1995]) to reliably identify asteroid families in a sample of 12,487 asteroids and throughout almost the entire belt. However, they also found that there are still some regions of the belt where a reliable identification of families was not possible. This could result from two main problems: either the proper elements in these regions were of degraded accuracy (e.g. near the resonances; see Milani and Knežević [1999] for an attempt to improve upon the accuracy of mean/proper elements of asteroids in the vicinity of the mean motion resonances), or the background density of asteroids was too high, thus smearing the family borders and forcing the clumping of families which should have been kept separate (this applies especially in the Flora region).

In addition, it has been recently recognized that chaotic diffusion, acting over very long time spans, can drive members of the families out of the regions in the phase space occupied by the families. Such a diffusive transport of the bodies seems to be common if a family is cut through by some mean motion resonances, giving rise to chaotic behavior localized to a narrow range of semiamjor axis (Milani and Farinella [1994], Milani et al. [1997], Morbidelli and Nesvorný [1999]). Another efficient mechanism of "family erosion" is provided by the Yarkovsky effect, which also appears to transport some family members out of the families by pushing them into the nearby resonances (Vokrouhlichký et al. [1999]).

In an attempt to solve the problem, and to produce proper elements more accurate, more stable in time and more reliable, we have tried a different method to compute asteroid proper elements. We adopted an approach similar to the one used for the major outer planets by Carpino et al. ([1987]): by purely numerical techniques, we produced so-called "synthetic" proper elements for a large sample of asteroids. The procedure consists of simultaneous integration of the asteroid orbits for a "long-enough" time span, online filtering of the short-periodic perturbations and computation of Lyapunov Characteristic Exponents to monitor the chaotic behaviors. The output of the integration is then spectrally resolved under constraints set by d'Alembert rules, and the principal harmonics (proper values) extracted from the time series, together with the associated fundamental frequencies.

It is quite obvious that with such an approach we have to handle in different ways the inner and the outer part of the main belt. In the outer part of the belt we are allowed to use a somewhat simplified dynamical model:

the direct perturbation are included only for the four outer major planets, while a barycentric correction applied to the initial conditions removes most indirect effects of the inner planets (Milani and Knežević [1992]). In this way we could speed up the numerical integrations by choosing a longer step size. In the inner part of the main belt, on the other hand, we have to include the effects of the terrestrial planets (at least Mars and Earth), and this makes the model more complex and significantly slows down the integration.

In this paper we present the results of the first phase of this work, that is the results of computation of the synthetic proper elements for a total of $10,265$ asteroids located in the outer main belt, between 2.5 AU and 4.0 AU. We propagated all the orbits for 2 Myr, but in a number of troublesome cases we extended the integrations to 10 Myr. We have included in this catalog only numbered and multi-opposition objects, to be sure that their osculating orbital elements are accurate enough; there would be no point in producing proper elements with a computational accuracy better than the one of the available osculating elements. We have also excluded the high eccentricity Mars approachers, that is those with initial perihelion $q < 1.75$ AU, because for these the perturbations by Mars should be taken into account.

The rest of the paper is organized as follows. In Section 2 we explain what is a synthetic theory, describe the procedures involved, the input data, and other important details and technicalities; in Section 3. we present and discuss the results, with special emphasis on the hyperbolic, resonant and chaotic cases, and we asses the accuracy and stability of the synthetic proper elements we have computed. We also give some examples of the new features, of the dynamical structure of the entire belt and of some families, which are made visible by more accurate and reliable proper elements. Finally, in Section 4 we summarize the results, draw some conclusions, and discuss future work.

2 Synthetic theory

The idea to develop a theory of motion by means of a set of purely numerical procedures is not new, but so far it has been used in the Solar System dynamics only for subsystems with a few bodies. The numerical approach was used as a complement to the analytical one, to integrate an analytically defined secular system (Laskar [1988]), or even to develop a fully numerical theories of motion, but for the systems with fewer bodies. The first long-term direct numerical integrations of the equations of motion of the Solar System were made by Cohen and Hubbard ([1965]), who integrated five outer planets for $120,000$ yr. This integration was later extended to 1 Myr by Cohen et al. ([1973]), and to 5 Myr by Kinoshita and Nakai ([1984]). As the computing power increased over the last couple of decades, the time span covered by integrations has also expanded, and Applegate et al. ([1986]), using a dedicated "Digital Orrery" computer, integrated orbits of the outer planets for more than 200 Myr, and later for even more.

In the framework of the LONGSTOP project (Milani et al. [1987], Carpino et al. [1987], Nobili et al. [1989]) *synthetic* (as opposed to analytic) theories of motion of the outer planets were derived by means of a set of purely numerical procedures, which consisted in the integration of orbits of the planets for 9.3 Myr, later 100 Myr, with online digital filtering to eliminate short-periodic perturbations, and Fourier analysis of the filtered output to identify the spectral lines. One advantage of such a procedure is that it allows a direct quantitative comparison with the results of analytic theories. This represents the core of the method applied in the present paper, although some adaptations to the asteroid case had to be done,

We computed proper elements for numbered and multi-opposition asteroids, with initial conditions taken from the *astorb.dat* osculating orbital elements data base for the epoch JD 2451100.5 provided by E. Bowell[1]. The reason to select only asteroids observed at multiple oppositions was that only for these objects the accuracy of orbital elements is sufficient to match the accuracy of the proper elements we wanted to compute.

2.1 Numerical integration

For the computation of highly accurate asteroid proper elements the numerical procedures involved, in particular the numerical integration, must also be as accurate and reliable as possible. For the purpose of our project, however, the choice of the integrator and the tuning of the parameters controlling the performance had to satisfy also another, practically opposite requirement, namely computational speed. This because we were to integrate thousands of orbits, computing not only the differential equations of motion, but also the corresponding variational equations to estimate maximum Lyapunov Characteristic Exponents (LCE); and this for a time span long enough to enable an

[1] `ftp://ftp.lowell.edu/pub/elgb/astorb.html`

accurate and efficient averaging out of both the short and the long–periodic effects.

For all these reasons we decided to make use of the ORBIT9 integrator (version 9c), developed by one of us (AM), employing different dynamical models in different regions of the asteroid main belt. For the integrations we present in this paper (of the orbits of asteroids located in the outer main belt) we used only four outer planets as perturbing bodies, applying the "barycentric correction" to the initial conditions in order to account for the major part of the indirect effect of inner planets.

The ORBIT9 propagator-interpolator is described elsewhere (e.g. Milani and Nobili [1988]); it uses as starter a symplectic single step method (implicit Runge-Kutta-Gauss), and a multi-step predictor performs most of the propagation; the latter has a constant stepsize h and uses only one evaluation of the right hand side of the equations of motion for each step. The states at the discrete steps are not interpolated, because the filter input interval is automatically selected to be a multiple of the step h. The latter is selected in an optimum way by using the estimates of the truncation error from Milani and Nobili [1988]. However, we have improved the algorithm for this stepsize selection by replacing the value of e in the corresponding equations by the value of $(e^2 + sinI^2)^{1/2}$, which is more predictive of the long term behavior of the eccentricity. In this way a suitable stepsize is computed for each asteroid. Then the input catalog is sorted by the stepsize and integrated in batches with similar stepsizes, by using the minimum of the recommended stepsizes.

We propagated the orbits of all the asteroids in the input catalog from the present state until 2 My in the past. Then proper elements were computed as discussed in Sections 2.3 and 2.4, and tested for stability in time as discussed there. For most asteroids the results turned out to be satisfactory; for the minority for which there were indications of instability and/or strong chaotic motion we performed a further integration from the initial state to 10 Myr in the future. The final proper elements catalog has been produced by joining the output files and replacing the 2 My results with the 10 My ones when available.

2.2 Digital filtering

The typical output of a long-term numerical integration of an orbit consists of the time series of orbital elements (and possibly other quantities) sampled at regular intervals, much longer than the time step of the integration itself.

This *decimation* of the output is in our case combined with the digital *filtering* to cut off the short-period perturbing terms. The N-body problem is strongly degenerate, that is the spectrum of the orbital elements is divided in two distinct regions, at high and low frequencies. This allows filtering to be performed independently from the Fourier analysis of the secular system, which by definition contains only the low frequencies. This requires to design filters with performances specifically adapted to the problem; some of the requirements are conflicting, and in practice a suitable compromise must be reached for an optimum performance.

The digital filtering procedure applied in the present paper is described in detail in Carpino et al. ([1987]). Thus we only briefly outline the algorithm and the particular choices of the main parameters. The output of the numerical integration can be represented as a time series of orbital elements sampled at regular intervals of length T_s; for a generic element x

$$x_j = x(t_j) \quad (t_j = t_0 + jT_s,\ j = 0, 1, 2, \ldots)\,.$$

In order to produce a correct spectral representation of the time series, it is necessary to take into account that the *discrete Fourier transform* of the signal

$$\hat{x}(\omega) = \sum_{k=-\infty}^{+\infty} x_k \exp(-ik\omega\, T_s) \quad (i = \sqrt{-1})$$

is periodic with period equal to the *sampling frequency* $\omega_s = 2\pi/T_s$

$$\hat{x}(\omega) = \hat{x}(\omega \pm k\omega_s), \quad k = 1, 2, \ldots$$

and therefore any spectral line having frequency $|\omega| > \omega_s/2$ will generate a *low frequency alias* in the region $[-\omega_s/2, \omega_s/2]$, more precisely at the frequency

$$\omega_{\text{alias}} = \omega - k_a\omega_s, \qquad \text{where } k_a = \text{int}\left(\frac{\omega}{\omega_s} + \frac{1}{2}\right)\,.$$

Of course, this situation is highly undesirable, because the interpretation of a spectrum in which real features are mixed with aliased lines would be difficult. In order to avoid this, it is necessary to use a sampling periodicity T_s satisfying the so-called *Nyquist criterion*, according to which the sampling frequency ω_s must be larger than $2\omega_{\max}$, where $\omega_{\max}$ is the highest frequency present in the spectrum of the series.

In the case of the output of the numerical integration of planetary orbits, this would mean to sample the orbital elements at least several times per revolution of the body having the shortest orbital period, in order to avoid aliasing from the short periodic terms produced by its perturbation. For a long-term integration, the adoption of such a short sampling periodicity would in turn produce a huge amount of output: this is not only demanding from the point of view of the computer resources, but would also make the subsequent steps of analysis of the results very cumbersome; on the other hand, if one is interested only in the long-periodic features of the spectrum, the information about short periodic terms is anyway not necessary.

A possible solution of this problem consists in the cancellation of the high frequency components of the signal by appropriate *digital filtering* techniques; after the application of a suitable *low-pass* digital filter removing all short-periodic terms, the sampling periodicity of the output can be reduced substantially without generating aliasing. Basically the filtering procedure consists in a *linear convolution* of the time series of the orbital elements x_j with a suitable finite real succession d_k:

$$y_m = (d * x)_m = \sum_{k=-M}^{+M} d_k \, x_{m-k} \, ;$$

in this way the spectrum of the convolved signal $\hat{y}(\omega)$ is equal to the product of the spectrum of the input signal $\hat{x}(\omega)$ and the *frequency response* of the filter $\hat{d}(\omega)$ (which is the discrete Fourier transform of the filter coefficients d_k); the filter can be designed in such a way that its frequency response is almost zero for frequencies larger than a prescribed *cutoff frequency* ω_{cut}

$$|\hat{d}(\omega)| \simeq 0 \qquad (\text{for } |\omega| > \omega_{\mathrm{cut}})$$

For the filtered signal y_j the Nyquist criterion becomes

$$\omega_s = \frac{2\pi}{T_s} > 2\omega_{\mathrm{cut}} \, ;$$

of course, in the actual design of the filter, ω_{cut} must be selected in such way as to preserve the spectral features of interest (in our case, the region of the spectrum corresponding to secular terms).

For the computation of synthetic proper elements, we have used a filter with decimation 100; e.g., in our 2 Myr integrations, we have used an input sampling frequency of one data point every 2 yr, and the output contains one data point every 200 yr. Long frequency aliases can be produced, as a result of

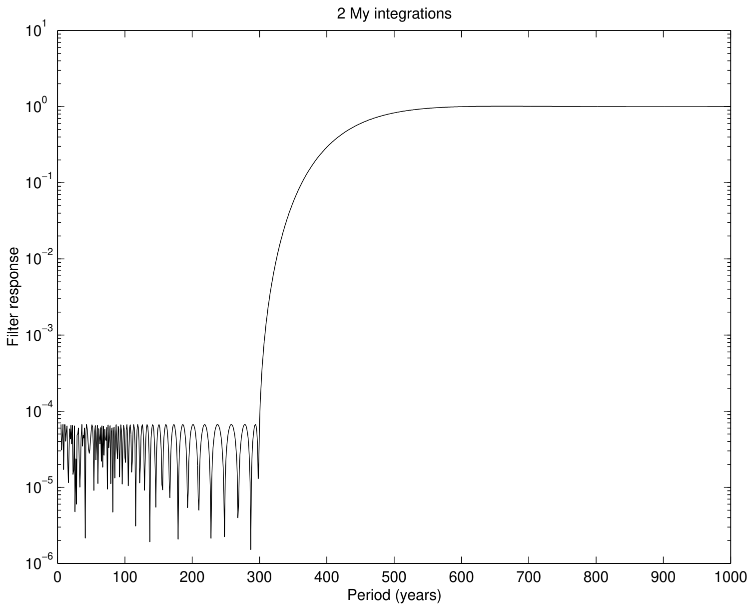

Figure 1: Frequency response of the digital filter, as used in the 2 Myr integrations.

a beat with the input frequency, only if they have periods less than the input Nyquist period of 4 yr; thus, in the outer asteroid belt, the perturbations with a frequency close to the mean motion cannot be responsible for spurious long periodic terms.

The frequency response of this filter is shown in Figure 1, in particular the dark band is for periods up to $\simeq$ 300 yr with response $|\hat{d}(\omega)| < 10^{-4}$, and the pass band is for periods above $\simeq$ 720 yr with response $0.999 < |\hat{d}(\omega)| < 1.001$. In this way the short periodic perturbations are removed from the filtered output, while the secular perturbations are not significantly distorted. Note that the response at zero frequency is $\hat{d}(0) = 1$; this implies that the long term average is preserved. Moreover, the coefficients of the filter we are using are symmetric, that is $d_m = d_{-m}$. In case the filter is applied to an angle variable, provided the angle time series is transformed into a continuous real function by adding 2π times the number of revolutions, the filter output has the same long term slope and phase of the original data. This is essential to be able to use the filter output to fit frequencies and phases. For the 10 Myr integrations, to avoid excessive output, we have used the same filter with one input data point every 5 yr.

2.3 Fourier analysis

The procedure to extract proper eccentricity and inclination, and the corresponding proper frequencies, is a modified form of Fourier analysis, which is adapted from the synthetic theory method introduced in Carpino et al. ([1987]), and further improved by Milani ([1993, 1994]).

The procedure includes three steps. First, the forced secular perturbations, which have known frequencies, are removed from the filtered time series for the equinoctal elements $k = e\cos\varpi, h = e\sin\varpi$ and $q = \tan(I/2)\cos\Omega, p = \tan(I/2)\sin\Omega$. Given the fundamental frequencies g_5, g_6, g_7 of the precession of perihelia of Jupiter, Saturn and Uranus respectively, we remove the Fourier components with these frequencies from (k, h). Given the fundamental frequencies s_6, s_7, s_8 of the precession of the nodes of Saturn, Uranus and Neptune respectively, we remove the Fourier components with these frequencies from (q, p).

Second, we compute the time series of the free arguments ϖ_f, Ω_f of the oscillation in the planes (k, h) and (q, p) respectively. This is done by computing the polar angles in these two planes, by adding multiples of 2π to obtain a continous function. Finally by a linear least squares fit we obtain an estimate of the proper frequencies g, the slope of ϖ_f, and s, the slope of Ω_f.

Third, we perform Fourier extraction of the proper mode. This can be done in two ways, as discussed in Milani ([1994]). Either the Fourier component with period $2\pi/g$ is extracted from the time series $(k(t), h(t))$; or the component with period 2π is extracted from the data expressed as functions of ϖ_f, that is $(k(\varpi_f), h(\varpi_f))$. The results would be identical if the proper oscillation was a linear one, but for non negligible eccentricity the higher order terms are important (Milani and Knežević [1990]) and the latter algorithm leads to more stable proper elements; thus we have used it. The same applies to the inclination related plane, and we have used the extraction of the component with period 2π from $(q(\Omega_f), p(\Omega_f))$. The amplitudes of these proper modes are the proper elements e_p and $\tan(I_p/2)$; the latter is then converted to the more usual $\sin I_p$.

One of the main advantages of the synthetic method is the availability of a stability test for each single set of proper elements computed in this way. In our previous work, with analytical proper elements, we needed specific numerical tests to check the stability of the results in a few supposedly representative examples; e.g., in the paper Milani and Knežević ([1994]) we tested only 35 asteroids.

In the computation of synthetic proper elements, a numerical integration over a long enough time interval $[0, T]$ has to be performed. Given the output of the same integration, the same algorithm described in this Section can be applied to shorter time intervals $[t_j, t_j + \Delta T]$, beginning at initial times $t_j, j = 1, .., N$, in such a way that $t_1 = 0$, $t_N = T - \Delta T$. For each of these "running boxes" a value of the proper elements $e_p, \sin I_p$ and of the proper frequencies is obtained, and the dispersion of these N values can be used to estimate the stability in time of the results. As an example, for the 2 Myr integrations we have used $N = 11$ running boxes of length $\Delta T \simeq 1$ Myr; for the 10 Myr integrations, $N = 9$ and $\Delta T \simeq 2$ Myr. The dispersion of the values of some proper element E in the different boxes can be measured by the root mean square σE (of the differences of the values computed in each box (with respect to the value computed over the entire time span) and by the maximum difference ΔE among the values computed in all the boxes.

2.4 Semimajor axis and Lyapunov exponents

The other proper element is proper semimajor axis a_p, which in principle is obtained by removing the short periodic perturbations from the time series of the osculating a. A rigorous definition would be somewhat more complicated than just the average of $a(t)$, because of second order perturbations which contain both constant and long periodic terms (Milani et al. [1987]). However, the second order perturbations are very small and in practice they are seldom the main source of time variation of the proper semimajor axis: chaotic effects are dominant in most cases. For this reason we have not attempted to perform second order corrections, and we have computed a_p as the mean of the values of $a(t)$ as it came out of the digital filter; that is, we are taking a mean of the already smoothed data. Stability tests are done again by the running box method.

There is a third proper frequency, f_p, which is the slope of the angle $\lambda = \ell + \varpi$. Note that in our numerical integration code the output for λ includes the principal value in $[0, 2\pi]$ and the number of revolutions completed since the initial conditions, thus the value of f_p can be obtained by a simple linear fit to the filtered λ; the filter also preserves the number of revolutions. Stability of f_p is tested by the running box method. In principle we can define a "mean mean motion" $n_p = f_p - g$ as the proper frequency of the mean anomaly ℓ. However, the frequency n_p is not related to a_p by Kepler's third law. This because the mean anomaly contains not only perturbations acting through changes in a, but also because of the accumulated effect of the perturbations in a (this is the classical double integration argument). In practice large deviations of λ from $f_p * t + \lambda_0$, let us say several revolutions, are a strong indication of chaotic motion (Milani et al. [1997]), in particular of jumps between different chaotic states corresponding to different values of a_p. For this reason we also use, as indicator of irregular motion, the root mean square and the maximum difference of the residuals of filtered λ with respect to the linear fit.

A well known indicator of chaotic motion is the maximum Lyapunov Characteristic Exponent (LCE). Although the LCE is rigorously defined as a limit for $t \to \infty$, an indicator can be obtained by a finite integration of both the equation of motion and the corresponding variational equation. Following Milani and Nobili ([1992], we compute an approximation of the LCE as the best fit slope of the function of time $\gamma(t) = \log[D(t)/D(0)]$, where $D(t)$ is the length of a variation vector (with initial conditions selected at random). Renormalisation of the variations vector needs to be applied when it becomes too large, to avoid numerical instability and overflow. This method typically allows to detect a positive LCE after 7-8 Lyapunov times T_L (T_L is the inverse of the LCE). The approximate values of the LCE computed in this way are reliable as order of magnitude, unless a real state transition between two chaotic regions takes place; the exact values are not very significant, changes by 20% when the integration time span is extended are typical.

3 Results

The results obtained with the new method to compute asteroid proper elements can be better described by distinguishing the stable and the unstable orbits. A large majority of the 10,265 initial conditions correspond to ostensibly regular orbits (at least over the tested time span), and for these we could determine synthetic proper elements with very good accuracy and stability in time: e.g., in 76% of the cases e_p and $\sin I_p$ had standard deviations (in the running box test) less than 0.001, and a_p less than 0.0003 AU. In 55% of the cases the RMS was even less than 0.0003 in e_p and less than 0.0001 in $\sin I_p$ (see Section 3.3). The typical improvement with respect to the analytically derived proper elements is by a factor of more than 3. In terms of the so-called *standard metrics* (Zappalà et al. [1990]) used to define asteroid families, this would imply a typical error of the relative velocity of family members with respect to the "parent body" on the order of ≈ 5 m/s (to be compared with ≈ 17 m/s for the analytical results).

On the other hand, in the basic 2 Myr run 9% of the cases had the standard deviations of either e_p or $\sin I_p$ larger than 0.003, 5% where chaotic with Lyapunov times shorter than $10,000$ yr (Section 3.3). At the extreme end of the stability/instability spectrum, we detected 31 "pathological" cases for which the changes with time of the proper elements and/or frequencies were excessively large, thus the values as given in the output are unreliable (Section 3.2). In 9 cases the orbits become hyperbolic, as a result of close approaches to some major planets, and of course we could not derive proper elements at all (Section 3.1).

For all the asteroids in our input catalog, with the only exception of the hyperbolic orbits, we have produced proper elements and error estimates as described in Section 2. These data are available online in three separate files: prop.syn, sigma.syn, and delta.syn, containing the proper elements, their standard deviations and maximum excursions, respectively, plus some additional information (LCE's, run code, RMS of residuals for the mean longitude linear fit). They are available from the web site `http://newton.dm.unipi.it` .

3.1 Hyperbolic cases

Let us begin with the most unstable orbits, that is with those that already during the 2 Myr integration became hyperbolic (see Table 1, upper part). For these 9 escaping asteroids it was not possible to determine synthetic proper elements, and they are removed from the output files. 14 additional bodies became hyperbolic in the extended 10 Myr integration (Table 1, lower part). For the sake of completeness, for these bodies we report the synthetic proper elements derived from the 2 Myr integrations, even if these values are highly unreliable and should be considered with extreme caution. Note that we thus provide proper elements for a total of $10,256$ asteroids.

[Table 1.]

We have not performed a detailed analysis of the reasons for such extreme instability. However, as it can be seen from the Remark column in Table 1, most of these orbits are from the start either inside or very close to some low order mean motion resonances, such as 2/1, 5/2, 7/3 and 9/4. Most of the others have a large initial eccentricity, the only exception being one case in the most unstable portion of the outer belt, with $a \simeq 3.8$ AU.

The leakage to hyperbolic orbits from the belt that we found, which is due to gravitational perturbations only, can be extrapolated to get an estimate of the total loss over the age of the Solar System. If we extrapolate linearly from 9 bodies lost in 2 Myr, we could have as much as $20,000$ bodies lost over 4.5 Gyr. If we extrapolate from the 10 Myr integration, with 23 orbits going hyperbolic, that is 0.2% of the considered sample, we could have $\simeq 10,000$ lost over the age of the solar system. Even if this oversimplified computation does not take into account the size of the original population, its collisional evolution, or any other refinement, it clearly demonstrates that this is by no means a negligible phenomenon, and that the original number of asteroids must have been significantly larger than the present one.

3.2 Resonant and "pathological" cases

Another group of troublesome cases is more heterogeneous. It again consists mostly of resonant asteroids, but there are also a few asteroids for which the determination of some proper value(s) was seriously deteriorated due to other reasons. The approach we adopted for these bodies is based upon the idea that all the data which could have been computed with a reasonable accuracy might be useful at least for statistical purposes; therefore, we decided to keep all these bodies in the files, correcting only a few of them in a special way, whenever this was necessary.

It is obvious that some dynamical features (e.g. mean motion and secular resonances) limiting the accuracy of the analytical theories correspond to real effects in the exact dynamics, and therefore have to appear also in the numerical integration output. Thus the derived elements are as good as they can be, given that the definition of proper elements must be uniform to satisfy the basic requirements of the family identification procedures. Our synthetic theory makes use of the averaging principle, which is well known not to work for resonant asteroids. As a typical example of the outcome of an inappropriate application of averaging, and of the "erroneous" definition of a proper element, let us mention the Griqua group of asteroids, located in the $2:1$ mean motion resonance with Jupiter. As can be seen in Figures 7 and 8 (Section 3.4), all these bodies appear at the libration center, that is, as if they all had the same proper semimajor axis of $\simeq 3.28$ AU. Thus, even if these bodies are kept in the files, one should not use these averaged semimajor axes for family identification purposes.

A well-known solution to the problem of resonant asteroids is to adopt some other proper value, taking into account the resonance in its very definition, instead of the usual one. For example, the libration amplitude of the semimajor axis could replace the averaged semimajor axis (see, e.g., Milani [1993]), but then the question is how to use different proper elements (of presumably different accuracy) in the family identification procedure. Even if the bodies are only close to a strong resonances the accuracy of the determination of proper elements is degraded and the same problem applies (see Milani and Knežević [1999], for an attempt to improve upon this situation). Another approach is to compute special "resonant proper elements" (Morbidelli et al. [1995]), but these do not belong to the same 3D-space; such proper elements can be very useful locally (to study dynamics), but cannot be used for large scale structure (to identify families) because of the discontinuities and/or topological changes. Let us just mention here that we shall later (Section 3.5) revisit the problem of resonant asteroids, to discuss the leakage of asteroid families members due to chaotic diffusion along the resonances.

There are other reasons why synthetic proper elements and frequencies have been poorly determined in some special cases. For asteroids with very low eccentricities and high inclinations ($\sin I \geq 0.3$) two problems simultaneously affect the computation of proper elements. In the real dynamics, strong secular resonances (with frequencies either $g - g_5$, $g - g_6$, $g - g_7$ or $2g - 2s$ near zero) affect the determination of the proper values. At the same time the argument of the proper mode may be difficult to compute from the time series $(k(t), h(t))$ because the point (k, h) may sometimes be too close to zero. Both effects combine in an inaccurate computation of the proper frequency g; the proper value e_p is nevertheless accurate. For example, this appears to be the case with the asteroid 1991 UC, which has so low proper eccentricity ($e_p = 0.0031$) that an automatic computation of the proper longitude of perihelion was not possible. However, we have not performed any "manual intervention" of this kind, both because it would necessarily introduce subjective choices and because it would make our procedure impossible to use in the context of an automated informations service (such as NEODYS, see `http://newton.dm.unipi.it/neodys/`).

Some other cases of inaccurate computations of proper elements and/or Lyapunov exponents are the result of very chaotic motion and macroscopic instabilities. As an example, for asteroids 3480 and 1998 OP12 the computation of the Lyapunov Characteristic Exponent ended up with a numerical overflow. For 3480 the proper semimajor axis was determined with a very large error (see Table 2), and since the orbit became hyperbolic in the extended integration (Table 1), this simply means that the divergence of nearby orbits is at some times so rapid that more frequent renormalisation should have been used. Hence, we kept the proper elements of 3480 in the file, but with the proper values coming from the shorter integration, and with its LCE set to a conventional high value. 1998 OP12 has been removed from the proper elements file because it became hyperbolic already in the shorter integration (Table 1). For the asteroid 1991 QG a numerical overflow occurred in the 10 Myr integration for the maximum excursions of the nodal frequency and of the mean longitude residuals with respect to the linear fit (we simply set these two values to zero keeping the rest of the data). Note that the semimajor axis of this asteroid was very poorly determined even in the short run (Table 2), and that it became even worse in the extended one. In this case, again, we are dealing with a strongly chaotic object (Lyapunov time on the order of few thousand years), and such oscillations are not unusual.

It is to be understood that we could not analyze in detail every troublesome case found by our automated procedure. Thus, for most of the bodies we could simply report the deteriorated quantities. We defined as "pathological" all the cases for which one or more of the following conditions were met:

$$\begin{array}{ccccc} \sigma a_p > 0.01 & \sigma e_p > 0.1 & \sigma \sin I_p > 0.03 & \sigma g > 10 & \sigma s > 10 \\ \Delta a_p > 0.01 & \Delta e_p > 0.1 & \Delta \sin I_p > 0.03 & \Delta g > 30 & \Delta s > 30 \end{array}$$

Here σ and Δ are standard deviation and maximum excursion; the statistics for frequencies of perihelion g and node s are given in arcsec/yr, these for the proper semimajor axis a_p in AU. In Table 2 we give a list of objects for which one or more of the proper values, as derived from the basic 2 Myr integration, exceeded the above thresholds.

[Table 2.]

For a comparison we show a similar table (Table 3) with the "pathological" data detected in 10 Myr runs. Here we have chosen to include only asteroids for which one or more of the proper elements had standard deviation in excess of the adopted threshold. In the final output there are additional 20 objects with "pathological" standard deviations in frequencies, 9 objects with maximum excursion in frequency above the critical value, and 73 objects for which the maximum excursions of elements were found to be above the adopted threshold.

[Table 3.]

As one can easily see from the table, not all of the asteroids with large standard deviations of proper elements listed in Table 2 appear again in Table 3 (3480, 6626, and 1984 LK because they went hyperbolic, but some, e.g. 1993 FB35, because the standard deviation of a_p was indeed improved). Many other bodies from Table 2 also do not qualify for the "pathological" category in the extended run (such as the numbered asteroids 531, 3579, 4915, 5330, 7598). The running boxes of the 10 Myr integration being 2 Myr, twice as long as the ones of the shorter integration, the decrease of the instability of some proper element indicates that averaging over an extended time span better removes some long periodic perturbation.

Overall, however, we found more "pathological" cases in the long run than in the short run. This could be expected since the deterioration occurred for some chaotic asteroids and for a number of asteroids near secular resonances, so that in a long run the perturbation builds up more effectively. As an example, it is not surprising that a number of members of the high inclination Pallas family originally discovered by Lemaitre and Morbidelli ([1994]) appeared in our Table 3. As a by–product of our analysis, we have identified 12 new potential members of this family: 5222, 5234, 8009, 1977 RD, 1981 EJ40, 1993 UT, 1993 VV7, 1994 PP, 1994 TA1, 1995 CT1, 1998 QX, 1998 QZ85. However, this is possibly not a complete list, also because a number of high eccentricity objects have been *a-priori* eliminated from our integrations due to the osculating perihelion distance criterion (Section 1).

3.3 Stability

As mentioned above, one of the principal novelties in the present approach was the derivation of accuracy estimates (standard deviations and maximum excursions) for every single body included in our computations. Having all these estimates available, it was straightforward to perform a simple statistical analysis of the outcome and to decide on the criteria by which certain bodies qualify for an extended integration.

In the basic 2 Myr run we found only 6 objects with standard deviation in proper sine of inclination larger than 0.01; we found a total of 300 of them with $\sigma \sin I_p > 0.001$, but also 8544 asteroids with $\sigma \sin I_p < 0.0003$ (this value corresponds to ≈ 5 m/s in relative velocity). The situation was, as expected from the theory, somewhat more complicated for e_p: no objects had a standard deviation larger than 0.1, and only few of them had $\sigma e > 0.05$, but we found 593 objects with $\sigma e > 0.01$, and 2040 of those with $\sigma e > 0.001$; at the same time there are 6687 cases where $\sigma e < 0.0003$ (≈ 5 m/s). For more than half of our sample, more exactly for 5848 asteroids, the two conditions $\sigma e_p < 0.0003$ and $\sigma \sin I_p < 0.0001$ were simultaneously fulfilled. These results indicate an average improvement in the accuracy of proper elements by a factor more than 3 with respect to the previously available elements computed by means of the analytical theory.

On the other hand we can look at the results in terms of reliability: in 8009 cases $\sigma a_p < 0.0003$, $\sigma e_p < 0.001$ and $\sigma \sin I_p < 0.001$ are simultaneously satisfied. This level of stability was also available for most asteroids from analytical computations, but we had no way to identify the cases in which this condition was violated, since tests were performed only on a few tens of cases.

On Figure 2 number frequency distributions of the standard deviations and maximum excursions of the synthetic proper eccentricity and (sine of) proper inclination are given as derived from the 2 Myr integrations. The figure illustrates what we have already stated above, that is, that for the large majority of the bodies proper eccentricity and inclination are determined with an exceptionally good accuracy.

Note that the numbers of objects in the bins corresponding to the largest value of the excursion are one or two order of magnitude larger than the numbers of bodies in the corresponding bins of the standard deviation plots. Even for a regular oscillation the maximum excursions are larger than the standard deviations (by a factor $2\sqrt{2}$); however, a much larger ratio between excursion and standard deviation indicates that the proper value changes abruptly, but only occasionally and for a comparatively short time.

It is quite obvious that in many troublesome cases an extended integration might give better and/or more reliable results. For chaotic objects (see section 3.4), for example, in particular for the stable-chaos cases, an extended integration, implying different sampling and filtering, could perhaps provide

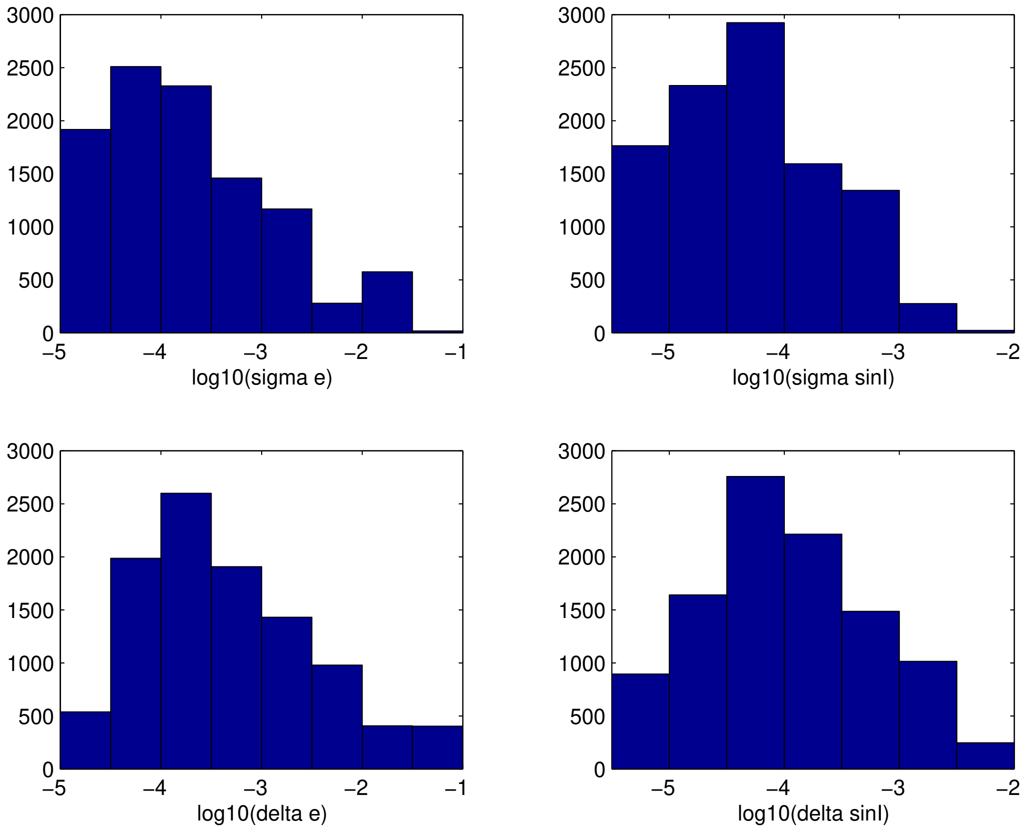

Figure 2: Number frequency distributions of standard deviations (up) and maximum excursions (bottom) of the proper eccentricity (left) and proper sine of inclination (right), as determined from the 2 Myr integrations.

results of improved accuracy. For objects affected by secular resonances with periods up to several Myr, again only an extended integration can provide enough data for a correct averaging, and so on. All these arguments had to be considered to select the orbits for which the integration should have been extended to 10 Myr. We adopted the following criterium:

$$\sigma a_p > 0.0003; \ \sigma e_p > 0.003; \ \sigma \sin I_p > 0.001; \ LCE > 5 \times 10^{-5}$$

These choices are slightly different from those used above to assess the quality of the proper elements; in particular, here we used also the LCE criterion, that is, we included also the chaotic objects. We found a total of 1860 objects meeting at least one of these conditions, and thus qualifying for a 10 Myr

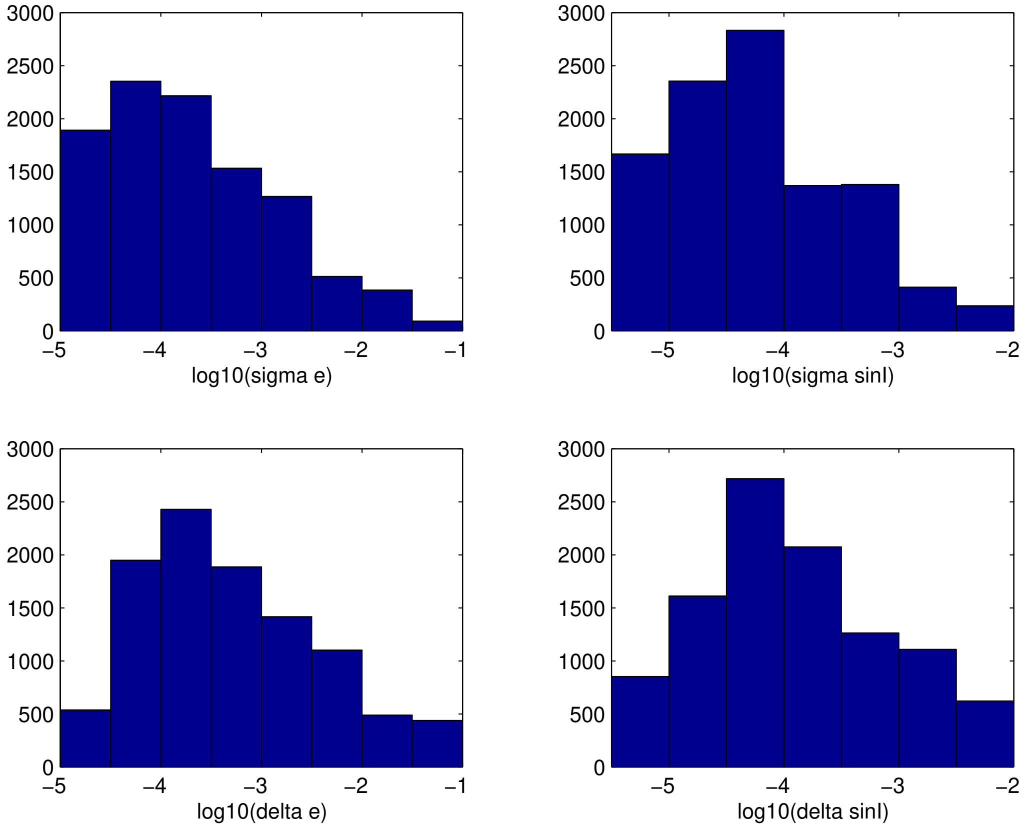

Figure 3: Number frequency distributions of standard deviations (up) and maximum excursions (bottom) of the proper eccentricity (left) and proper sine of inclination (right), with data from the joint catalog. Note an increase of the number of asteroids with large errors.

integration; this number represents an acceptable compromise between the need for extending as many orbits as possible and the available computing power.

The extended integration resulted in 307 "recovered" good results, that is asteroids with $\sigma a_p < 0.0003$, $\sigma e_p < 0.001$ and $\sigma \sin I < 0.001$ simultaneously satisfied. As already mentioned, 14 objects became hyperbolic; we found 1347 objects with $\sigma e_p > 0.001$, 642 objects with $\sigma \sin I_p > 0.001$, and 475 objects with $\sigma a_p > 0.0003$.

Eventually, the final catalog was formed by joining the two outputs, that is by replacing the 2 Myr output with the 10 Myr one for the asteroids for which the latter was available. Since in some cases the instability accumulates with time, this results in an increase of the number of cases with large instability (compare Figure 2 with Figure 3, and Figure 4 with Figure 5). For example out of 8009 proper elements sets rated as good in the 2 Myr run, 513 actually correspond to the chaotic objects ($T_L < 20,000$ yr); they have been included in the extended integration, exhibiting thereafter an apparent deterioration of the statistics simply because chaotic diffusion in the proper elements space had more time to act. In other words, the extended integration revealed a number of asteroids with poorly determined proper elements, and these results, even if apparently worse in terms of a simple minded statistics, are in fact better and more reliable.

Summarizing the final results we report 478 objects with $\sigma e_p > 0.01$ and 2259 with $\sigma e_p > 0.001$, 9 with $\sigma \sin I_p > 0.01$ and 650 with $\sigma \sin I_p > 0.001$. For 6382 asteroids we found $\sigma e_p < 0.0003$, for 6856 $\sigma \sin I_p < 0.0001$, and 5625 fulfilling both conditions. We found in 7804 cases all three standard deviations being good ($\sigma a_p < 0.0003$, $\sigma e_p < 0.001$ and $\sigma \sin I < 0.001$). In Table 4 we list all the above quoted, as well as some additional results (for other values of the standard deviations) on the three sets of data, while in Figure 3 we show number frequency distributions for the final joint output (to be compared with Figure 2).

Some questions could arise about the reliability of our estimates of the accuracy of proper elements for the asteroids whose orbits have been computed for 2 Myr only. Could some of these turn out to be more unstable over an extended time span? Out of $\simeq 10,000$ cases, it would be unwise to make an absolute statement that this could never happen. However, the orbits selected for the extended integration have been the ones already showing instability of the proper elements and/or chaotic behavior, and the others are less likely to become unstable after having already been regular over 2 Myr. Still, this cannot be guaranteed.

[Table 4.]

In Figures 4 and 5 we show the number frequency distributions of the semimajor axes standard deviation, of the mean longitude differences with respect to the linear fit, and of the maximum Lyapunov Characteristic Exponents (LCE). In addition, there is are plots of LCE vs. proper semimajor axis to reveal the chaotic regions in the outer main asteroid belt. The latter plots are similar to the one produced by Morbidelli and Nesvorný ([1999]; Figure 1), but ours are produced with the initial conditions of real objects,

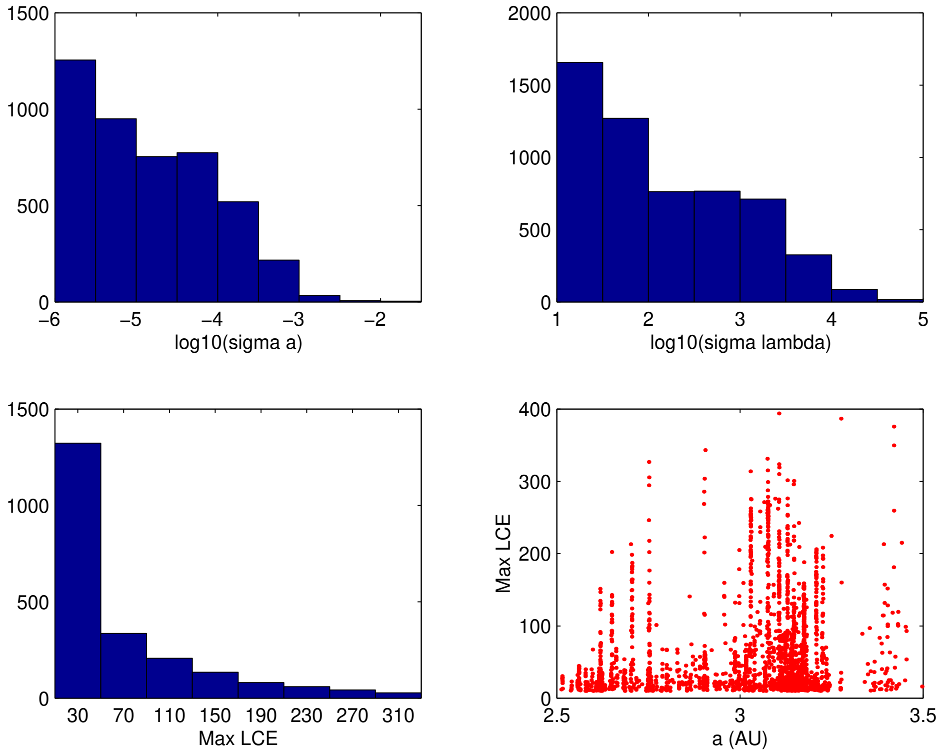

Figure 4: Upper plots give number frequency distributions of standard deviations of proper semimajor axis (left) and of the difference in degrees of the mean longitude with respect to the linear fit (right), as obtained in the 2 Myr integrations. Lower plots give for the same integration the number frequency distribution of maximum Lyapunov Characteristic Exponents (left), and LCE vs. proper semimajor axis (right).

rather than with fictitious initial conditions on a grid. It is easy to see that the regions of strongest chaos coincide with the main mean motion resonances, that the region between 3.0 and 3.2 AU hosts many moderately and strongly chaotic asteroids, and that, in general, these plots are qualitatively identical with those obtained in simulations. The largest maximum LCE of $\sim 5.6 \times 10^{-4}$ corresponds to $T_L \simeq 1800$ yr. The detailed statistics of LCE can be found in Table 4.

The chaos in the asteroid outer main belt is due mostly to the mean motion resonances (including the three–body ones; see Nesvorný and Morbidelli [1998]), and therefore the chaotic orbits are characterized by comparatively large irregular oscillations of the proper semimajor axes. These are quite

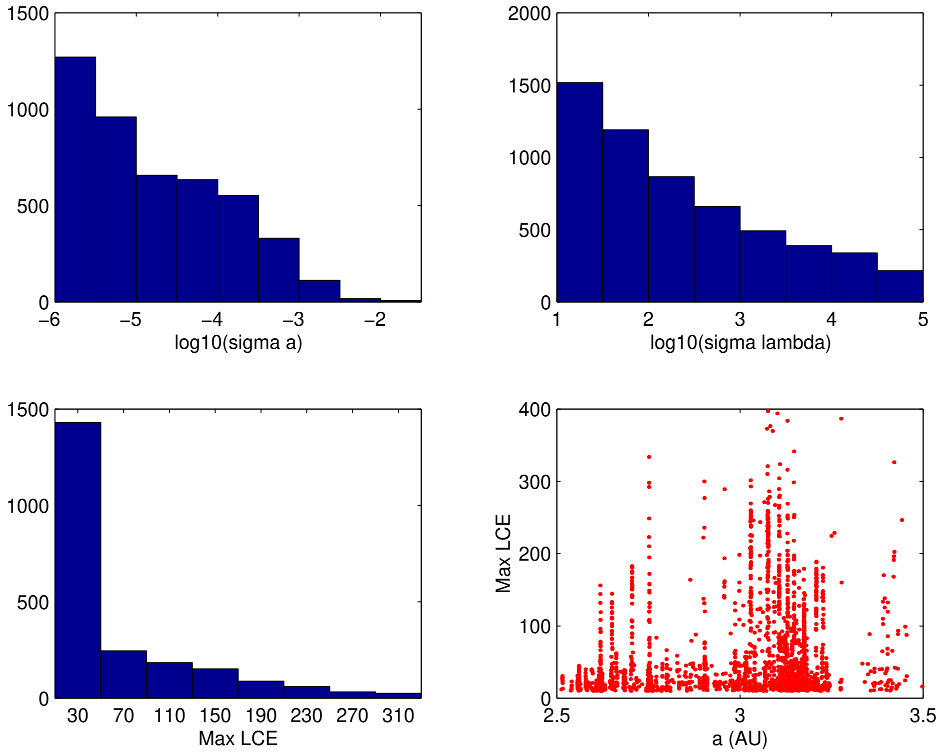

Figure 5: The same as Figure 4, but for the data from the joint catalog.

well known facts, and they are fully confirmed on Figures 4 and 5, as well as on Figure 6 showing a clear correlation between the maximum LCE and the standard deviation of the proper semimajor axis. In other words, both these quantities are quite sensitive indicators of chaotic behavior and can be used to detect and measure it. The statistics of the residuals of the mean longitude with respect to a linear fit can also be used as a very sensitive indicator of chaos, although its use is somewhat more difficult, because our theoretical understanding of its significance is incomplete.

The LCE data, as shown in Figures 4 and 5, do not change significantly between the 2 Myr integration and the 10 Myr one. This was expected, as even the shorter integration was long enough for a reliable determination of the maximum LCE for the strongly chaotic orbits with short Lyapunov times. Still, one can notice in Table 4 that the number of orbits with T_L less than $20,000$ yr is slightly decreased in the joint catalog with respect to the 2 Myr run; this because in the extended integration the maximum

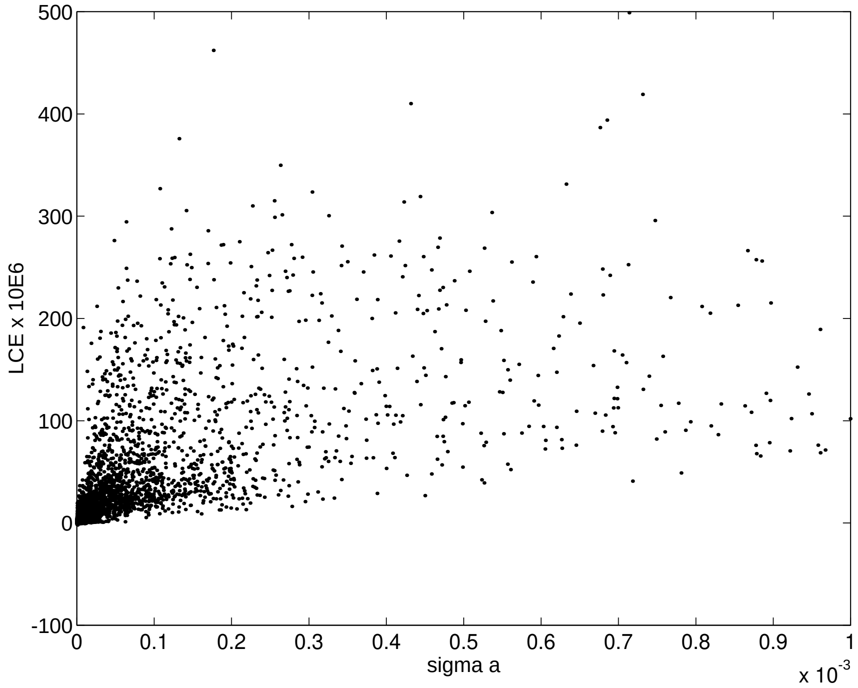

Figure 6: Maximum LCE and standard deviation of the proper semimajor axis. A clear correlation between these two indicators of chaotic motion is apparent. The largest values of σa are not shown.

LCE estimate was more accurately determined, especially for the moderately chaotic orbits. This resulted in somewhat lower estimates of the maximum LCE in the extended run, but, as a rule, of the same order of magnitude as that found previously.

3.4 Global view of the outer main belt

A global view of the outer main asteroid belt is given on Figures 7 and 8 in the (a, e) and $(a, \sin I)$ planes, respectively. Only asteroids with good proper elements are shown on these plots (the actual criteria were exactly opposite from those for the inclusion in the 10 Myr run, that is $\sigma a < 0.0003$, $\sigma e < 0.003$, $\sigma \sin I < 0.001$ and $LCE < 5 \times 10^5$). The plots are made with the data from the joint catalog.

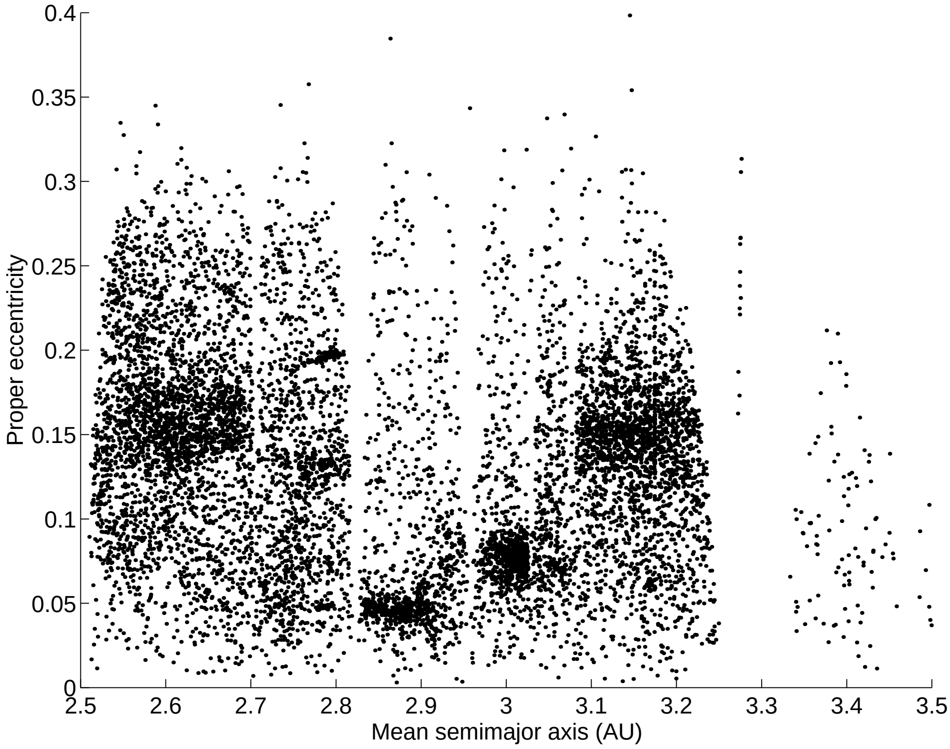

Figure 7: An overview of the asteroid outer main belt in proper semimajor axis vs. proper eccentricity plane. Only asteroids with accurately determined proper elements are shown.

A rather unexpected feature visible in Figure 8 is a "line" of objects at proper inclination $\simeq 0.37$ and with $2.6 < a_p < 2.7$ AU. These objects all have a low proper eccentricity, but only for a subset the values of e_p are in a narrow range, indicating a possible Hansa family (from 480 Hansa, the lowest numbered asteroid in this group). However, without more detailed study we cannot exclude that such grouping is only apparent, due to an island of stability surrounded by secular resonances.

In Figure 9 the troublesome cases are shown in the same planes (a_p, e_p) and $(a_p, \sin I_p)$. The chaotic asteroids (either $\sigma a > 0.0003$ or $LCE > 5 \times 10^5$) are shown on the left: these two plots illustrate again the fact that the mean motion resonances are the main source of chaotic behavior for main

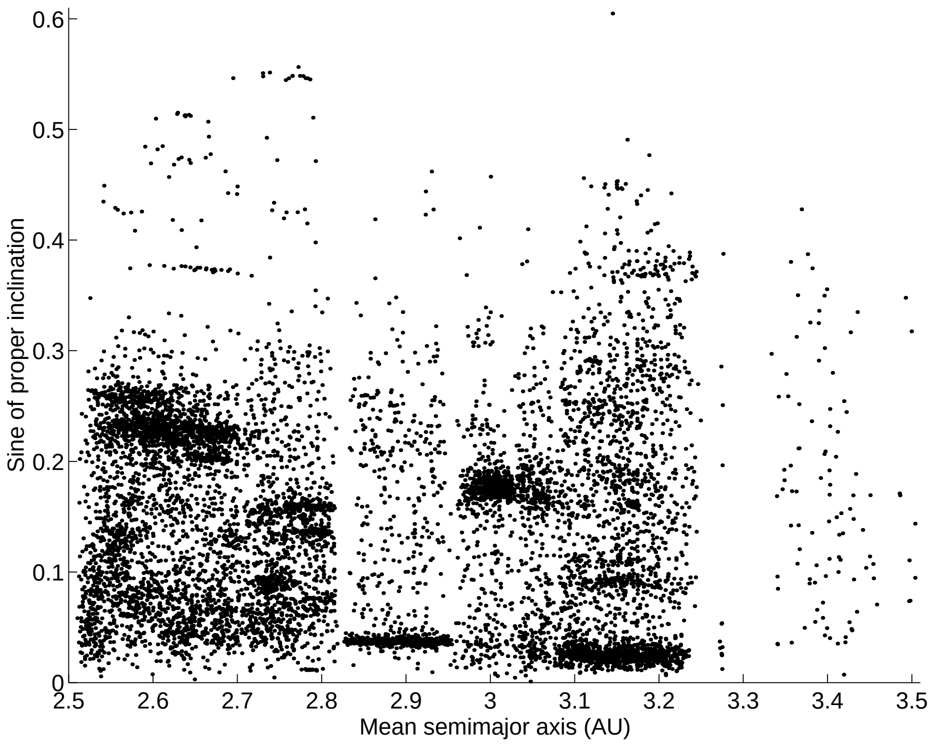

Figure 8: An overview of the asteroid outer main belt in proper semimajor axis vs. sine of proper inclination plane. Only asteroids with accurately determined proper elements are shown.

belt asteroids. The chaotic objects are distributed along numerous easily recognizable resonant strips; chaotic diffusion takes place along the resonance lines (see Section 3.5). The most affected region is between 3.0 and 3.2 AU, even if in that region there are also many fairly stable asteroids (see Figures 7 and 8) and the region does not appear to be a continuous chaotic sea.

On the right of Figure 9 we show the orbits affected by the secular resonances (either $\sigma e > 0.003$ or $\sigma \sin I > 0.001$). These two plots illustrate the effects of secular resonances, the most prominent feature being the outline of a group of overlapping nonlinear secular resonances between 2.5 and 2.8 AU, at low to moderate inclination and eccentricity. The location of these resonances as revealed by the numerical integration coincides with the analytical

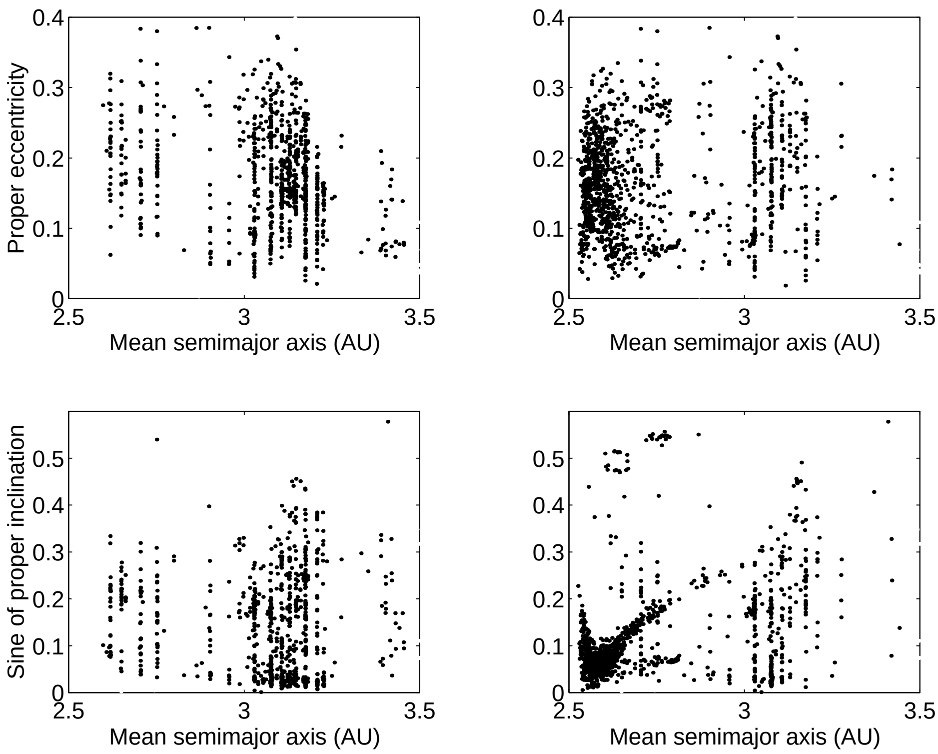

Figure 9: A composite figure showing chaotic asteroids (left) and asteroids with large standard deviations of eccentricity/inclination, affected by the secular resonances in the zone between 2.5 and 2.8 AU (right) in the proper semimajor axis vs. eccentricity (up), and semimajor axis vs. sine of inclination (bottom) plane.

prediction (see Figures 7–11 in Milani and Knežević [1994]). The numerical output not only indicates the exact location of these resonances, but can be used to estimate their width, providing in the same time a clear indication of the level of degradation of the proper elements due to the resonances themselves.

The comparison of the plots presented on Figure 9, which has been prepared with the composite catalog, with the analoguous plots produced with the data from the 2 yr run, shows an additional feature. Quite a number of objects found to be chaotic in the short run and thus appearing on the plots on the left, appear also on the other pair of plots on the right in the long run, even if the objects are not close to any significant secular resonance. As discussed above, chaotic perturbations affect immediately the semimajor axis, but on the long run chaotic diffusion also affects the other proper variables.

3.5 Families

The new set of synthetic proper elements is accurate enough to enable the study of the dynamical features of individual families. Such studies have been conducted in the recent past (e.g. family of Veritas; see Milani and Farinella [1994]; Milani et al. [1997]; Knežević and Jovanović [1997]; Nesvorný and Morbidelli [1998]; Knežević [1999]) in the framework of dedicated projects, but now one can recognize many interesting features by simply looking at suitably prepared plots. Many of these features, so far hidden and/or smeared out by proper elements not accurate enough, became visible due to better resolution provided by new elements.

The chaotic orbits are included in the family envelopes as projected on the $(a, \sin I)$ space, for example, especially within the largest families like Koronis, Eos and Themis, but also within the small, compact ones, like Hygiea and Veritas. Mean motion resonances cross the families giving rise to chaotic diffusion, and this causes the family members to spill out from the regions occupied by the families. Thus, even if genuine fragments belonging to the families (possibly billions of years ago), they do not belong to the family cluster as they can be identified with the present orbits. Such objects are crucial for the studies of the post-formation dynamics of fragments and could be counted in the family membership. On the other hand, they should not be used for the reconstruction of the breakup relative velocity fields, not to mix chaotic diffusion with relative velocities acquired at breakup.

As an example we show on Figure 10 the region in the (a_p, e_p) plane where the Koronis and Eos families are located. Some alignments of chaotic objects, possible ex-members of the families, along the resonant lines is clearly visible. The spillover from Koronis family due to chaotic diffusion seems to be responsible for at least part of the so-called Prometheus surge at ~ 2.9 AU, while the 9:4 resonance affects Eos at ~ 3.03 AU, with spillover both to higher and lower eccentricities (compare with Morbidelli et al., [1995]).

Another example is shown in Figure 11, where the region with $3.05 < a_p < 3.24$ AU and $\sin I_P < 0.1$ contains the Themis and Hygiea families and is crossed by several mean motion resonances. It is clear that the spillover from the Themis family can extend a long way.

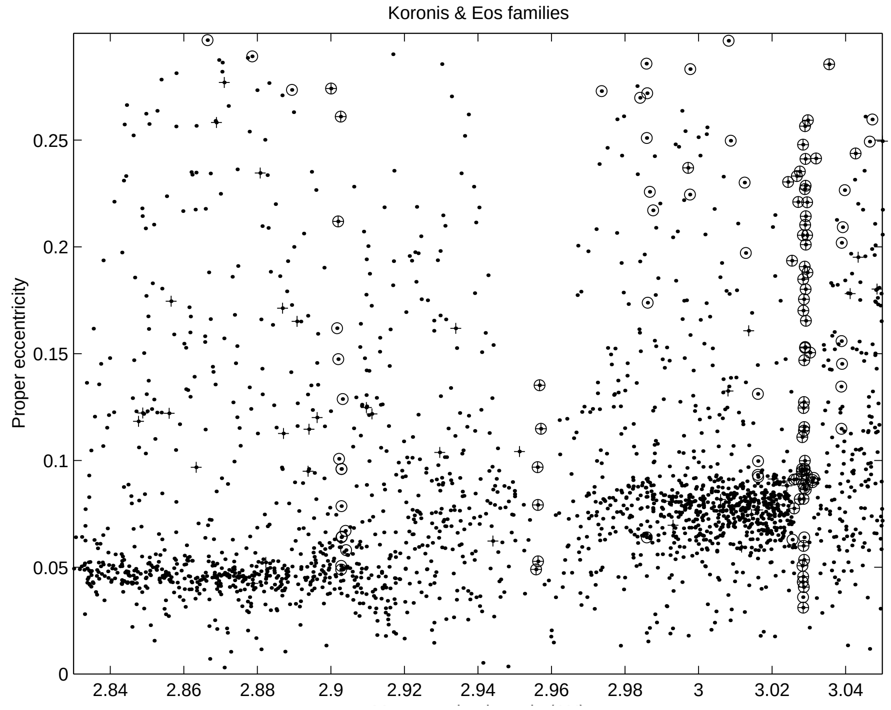

Figure 10: The region of the Koronis and Eos families. Dots stand for asteroids with good proper elements, crosses are objects with large errors in proper eccentricity and inclination; chaotic asteroids are marked with open circles – a dot inside the circle indicates stable chaos cases with satisfactory proper eccentricity and inclination, while a cross inside the circle indicates that chaotic diffusion disturbed also eccentricity and inclination.

4 Conclusions

Summarizing the main results of this paper, let us recall especially the following:

- we developed a new, purely numerical procedure for the computation of "synthetic" proper elements of asteroids, which consists in: (i) numerical integration of asteroid orbits in the framework of a realistic dynamical model, (ii) online digital filtering of the short-periodic effects, (iii) Fourier analysis to remove main forced terms and find proper modes with given arguments, and (iv) checking the accuracy by means of running box tests;

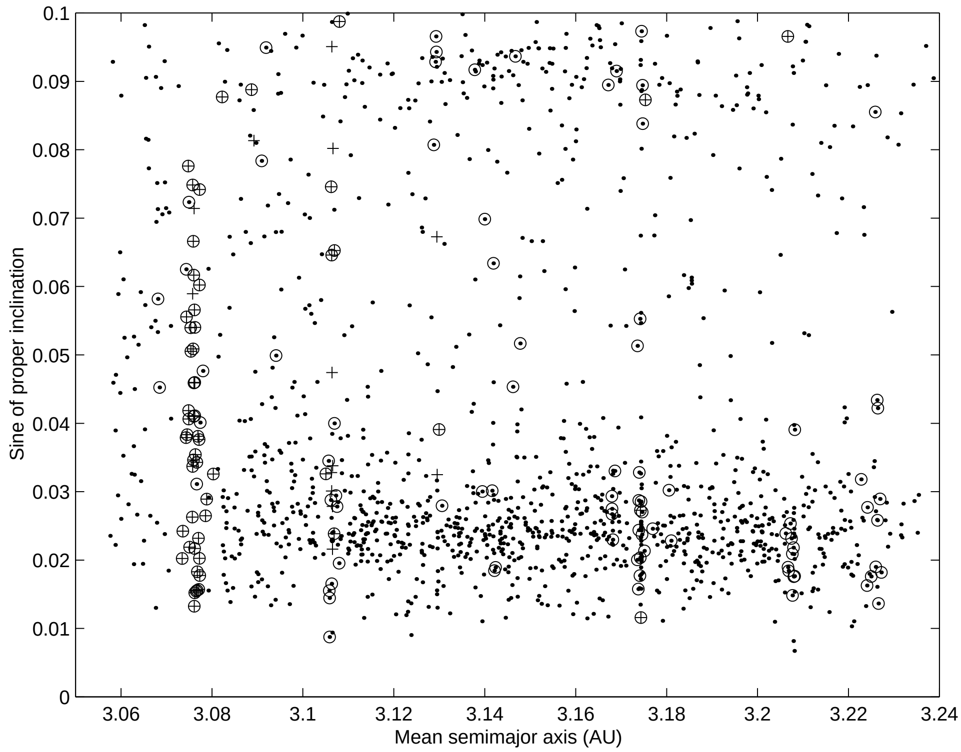

Figure 11: The region of the Themis and Hygiea families. Dots stand for asteroids with good proper elements, crosses are objects with large errors in proper eccentricity and inclination; chaotic asteroids are marked with open circles.

- by means of this theory, we produced a new set of accurate proper elements and frequencies for 10,256 outer main belt asteroids between 2.5 and 4.0 AU, combining outputs from the 2 Myr integration and from an extended 10 Myr integration, to which we subjected objects with proper elements/frequencies poorly determined in the shorter run;
- for each integrated body we provide an individual estimate of the accuracy of the results in terms of the standard deviations and maximum excursions, as well as an estimate of the maximum Lyapunov Characteristic Exponent; these data enabled us to conduct a comprehensive, yet straightforward statistical analysis of the results, and provided us with a sort of "dynamical portrait" of the outer main belt as a whole;
- we achieved an average improvement of the accuracy of new proper

elements with respect to previously available ones, computed by means of our analytical theory, by more than a factor of 3. In terms of the relative velocities at breakup this means that the typical accuracy is of the order of ~ 5 m/s.

- such a high accuracy of proper elements opens the possibility to study the individual families, their internal structure, boundaries and velocity fields, as well as the phenomena of chaotic diffusion, leakage of the members from the families, etc. In this respect, we offered few examples, including leakage along the resonant lines from Koronis, Eos and Themis families;

- the availability of individual measures of chaotic behavior for each asteroid provides a basis to study the dynamical structure of the entire region, from the point of view of the long-term stability of motion, e.g., in the Nekoroshev sense.

We would like to emphasize the implications of the availability of an accuracy estimate for each individual asteroid. This means that also the asteroids for which the proper elements are poor can be used in the study of asteroid families, but the users of the proper elements should take into account the uncertainty. The algorithm to do this has not yet been developed, but it is clear that the uncertainty must appear in the distances between sets of proper elements used for the classification procedures.

It is obvious that a wealth of data we produced contains plenty of information on the dynamics of the asteroids in the outer main belt, on the stability of their motion, chaos, families, and many other important topics. We plan in the next future to analyze some of these problems. In addition, we intend to extend our analysis to the inner part of the main belt (this will require inclusion of the terrestrial planets in the model and much more complex and time consuming integration/analysis), and to resonant asteroids such as Hildas and Trojans (with appropriately defined proper parameters).

On the contrary, we do not intend to consider Near-Earth objects (NEO's) in the framework of this project, as these have to be handled in a very different way (Gronchi and Milani [2000]).

Acknowledgements: We are grateful to M. Carpino for his kind assistance with the chapter on digital filtering. This research has been supported through the grants by the Italian Space Agency (ASI), by the Italian Ministry of Foreign Affairs and Yugoslav Ministry of Environment, Science and Development, and by the Ministry of Science and Technology of Serbia through the project 04M04 "Astrometrical, astrodynamical and astrophysical investigations".

References

[1986] Applegate, J.H., Douglas, M.R., Gursel, J., Sussman, G.J., and Wisdom, J.: 1986, The outer solar system fro 200 million years, *Astron. J.* **92**, 176–194.

[1963] Arnold, V.I.: 1963, Small denominators and problems of stability of motion in classical and celestial mechanics, *Russian Mathematical Surveys* **18**, 85–191.

[1987] Carpino, M., Milani, A., and Nobili, A.M.: 1987, Long-term numerical integrations and synthetic theories for the motion of the outer planets. *Astron. Astrophys.* **181**, 182–194.

[1965] Cohen, C.J., and Hubbard, E.C.: 1965, Libration of the close approaches of Pluto to Neptune *Astron. J.* **70** 10–13.

[1973] Cohen, C.J., Hubbard, E.C., and Oesterwinter, C.: 1973, *Astron. Papers Amer. Ephem. Naut. Alm.* **XXII**, part I.

[2000] Gronchi, G.F. and Milani, A.: 2000, *Proper elements for Earth crossing asteroids*, submitted.

[1984] Kinoshita, H., and Nakai, H.: 1984, Motions of the perihelions of Neptune of Pluto, *Cel. Mech. & Dyn. Astron.* **34**, 203.

[1999] Knežević, Z.: 1999, Veritas family age revisited. In: *Evolution and source regions of asteroids and comets* (J. Svoreň, E.M. Pittich, and H. Rickman, eds.), pp.153–158.

[1997] Knežević, Z., and Jovanović, B.: 1997, Is the chaotic clock ticking correctly? *Bull. Astron. Belgrade* **156**, 47–69.

[1988] Laskar, J.: 1988, Secular evolution of the solar system over 10 million years. *Astron. Astrophys.* **198**, 341–362.

[1989] Laskar, J.: 1989, A numerical experiment on the chaotic behaviour of the solar system. *Nature* **338**, 237–238.

[1994] Lemaitre, A., and Morbidelli, A.: 1994, Proper elements for highly inclined asteroidal orbits. *Cel. Mech, & Dyn. Astron.* **60**, 29–56.

[1993] Milani, A.: 1993, The Trojan asteroid belt: proper elements, stability, chaos and families. *Cel. Mech. Dyn. Astron.* **57**, 59–94.

[1994] Milani, A.: 1994, The dynamics of the Trojan asteroids. In: *Asteroids, Comets, Meteors 1993* (A. Milani, M. Di Martino, and A. Cellino, eds.), Kluwer Acad. Publ., Dordrecht, pp. 159–174.

[1994] Milani A., and Farinella, P.: 1994, The age of the Veritas asteroid family deduced by chaotic chronology. *Nature* **370**, 40–42.

[1990] Milani, A., and Knežević, Z.: 1990, Secular perturbation theory and computation of asteroid proper elements. *Cel. Mech. & Dyn. Astron.* **49**, 347–411.

[1992] Milani, A., and Knežević, Z.: 1992, Asteroid proper elements and secular resonances, *Icarus* **98**, 211–232.

[1994] Milani, A. and Knežević, Z.: 1994, Asteroid proper elements and the dynamical structure of the asteroid main belt, *Icarus* **107**, 219–254.

[1999] Milani, A. and Knežević, Z.: 1999, Asteroid mean elements: higher order and iterative theories, *Cel. Mech. & Dyn. Astron.* **71**, 55–78.

[1988] Milani, A., and Nobili, A.M.: 1988, Integration error over a very long time span. *Cel. Mech. & Dyn. Astron.* **43**, 1–34.

[1992] Milani, A., and Nobili, A.M.: 1992, An example of stable chaos in the Solar System. *Nature* **357**, 569–571.

[1987] Milani, A., Nobili, A. M., and Carpino, M.: 1987, Secular variations of the semimajor axes: theory and experiments. *Astron. Astrophys.* **172**, 265–279.

[1997] Milani, A., Nobili, A. M., and Knežević, Z.: 1997, Stable chaos in the asteroid belt. *Icarus* **125**, 13–31.

[1997] Morbidelli, A., and Guzzo, M.: 1997, The Nekhoroshev Theorem and the Asteroid Belt Dynamical System. *Cel. Mech. & Dyn. Astron.* **65**, 107–136.

[1999] Morbidelli, A., and Nesvorný, D.: 1999, Numerous weak resonances drive asteroids toward terrestrial planets orbits. *Icarus* **139**, 295–308.

[1995] Morbidelli A., Zappalà, V., Moons, M., Cellino, A. and Gonczi, R.: 1995, Asteroid families close to mean motion resonances: dynamical effects and physical implications. *Icarus* **118**, 132-154.

[1998] Nesvorný, D., and Morbidelli, A.: 1998, Three-body mean motion resonances and the chaotic structure of the asteroid belt. *Astron. J.* **116**, 3029–3037.

[1989] Nobili, A.M., Milani, A., and Carpino, M.: 1989, Fundamental frequencies and small divisors in the orbits of the outer planets. it Astron. Astrophys. **210**, 313–336.

[1999] Vokrouhlický, D., Brož, M., Farinella, P., and Knežević, Z.: 1999, Yarkovsky-driven leakage of Koronis family and the case of 2953 Vysheslavia. *Bull. Am. Astron. Soc.* **31(4)**, 1111.

[1990] Zappalà, V., Cellino, A., Farinella, P., and Knežević, Z.: 1990, Asteroid families I: identification by hierarchical clustering and reliability assessment. *Astron. J.* **100**, 2030–2046.

[1995] Zappalà, V., Bendjoya, Ph., Cellino, A., Farinella, P., and Froeschlé, C.: 1995, Asteroid families: search of a 12,487-asteroid sample using two different clustering techniques. *Icarus* **116**, 291-314.

Table 1: Upper part: asteroids that became hyperbolic in the 2 Myr integration. Lower part: additional bodies that escaped during the extended 10 Myr integration. Columns contain asteroid identifier, semimajor axis, eccentricity and inclination at the beginning of the integration, and comment on the relevant dynamical features that might give rise to chaotic diffusion. T_L denotes the Lyapunov time in years.

Asteroid	a_0 (AU)	e_0	I_0 (deg)	Remark
1921	3.263	0.402	19.45	2/1
5164	3.643	0.504	19.84	outer belt
7458	3.830	0.137	1.81	outer belt
8119	2.963	0.166	0.61	7/3
1988DX1	2.828	0.175	8.13	5/2
1989TT3	2.820	0.157	3.00	5/2
1993SG13	2.958	0.228	6.85	7/3
1993TC14	3.304	0.273	0.35	2/1
2202T-1	3.122	0.329	4.14	2/1 ?
677	2.962	0.044	8.47	7/3 $T_L = 6060$ yr
2658	3.076	0.290	9.32	
3480	3.045	0.283	3.76	
6626	3.025	0.388	2.12	9/4
7410	3.022	0.376	5.85	9/4
8560	2.959	0.068	13.38	7/3 $T_L = 6200$ yr
1984LK	3.115	0.386	6.55	2/1 ?
1990OB2	3.035	0.335	11.68	
1991WB	2.747	0.330	35.99	secular res.
1996EJ14	3.029	0.096	15.80	9/4
1998DD2	3.058	0.318	8.35	
1998KY30	3.203	0.190	14.29	2:1 $T_L = 6200$ yr
1998OP12	3.038	0.307	1.31	
1998QO47	3.085	0.340	6.17	

Table 2: "Pathological" cases for which some proper value(s) had very large errors in 2 Myr run. Columns contain asteroid identifica-tion, statistics found to be excessively large, and a remark on the specific dynamical features of the bodies. See text for explanation of notation and units.

Asteroid	Erroneous values	Remark
531	Δg	
759	Δg	
1263	σg; Δg	
3480	σa	
3579	Δe; σg; Δg	
4112	σg	
4915	Δa	
5222	Δg	
5330	$\Delta \sin I$; σg; Δg	
5765	σg	
6626	σa	
7306	σg; Δg	
7598	Δa	
8009	Δg	
1977RD	σg	
1979OA	$\Delta \sin I$	
1981EJ40	σg	
1981QN3	σg	2/1
1984LK	σa; σs; Δs	
1987UW	Δg	
1991QG	Δa	
1991UC	σg	e=0.0031
1993FB35	σa; σs; Δs	
1993QN	Δg	
1993UT	$\Delta \sin I$; σg; Δg	
1993VV7	Δe; σg; Δg	
1994TA1	σg; Δg	
1995SU32	σg; Δg	
1998QX	Δe; σg	
2705P-L	Δa	
3230T-2	σg	2/1

Table 3: The same as Table 2, but for the 10 Myr integration. Included are only objects with excessive standard deviations of proper elements.

Asteroid	Erroneous values	Remark
1301	σe; σg	Pallas
4177	$\sigma \sin I$	2:1
4997	σe; σg	$g = s$; Pallas ?
1979OA	σe; σg; σs	$g = g_6; T_L \approx 4500$
1981EJ40	σe; σg	Pallas
1991QG	σa; σg; σs	$T_L \approx 6000$
1993SQ3	σa; $\sigma \sin I$; σg	2:1
1993TC23	σa; σg	$T_L \approx 6300$
1993UT	σe; σg	Pallas
1995CT1	σe; σg	Pallas
1996KL1	σa	$T_L \approx 2500$
2705P-L	σa	$T_L \approx 11000$

Table 4: Comparative analysis of the outputs: 2 Myr integration (10256 asteroids), 10 Myr integration (1846) and joint data (10256). The last row corresponds to $\sigma a < 0.0003$ & $\sigma e < 0.001$ & $\sigma \sin I < 0.001$.

Statistics		-2	10	joint
σa	> 0.001	45	131	138
	> 0.0003	273	475	488
	> 0.0001	781	823	1022
	> 0.00003	1592	998	1691
σe	> 0.01	593	472	478
	> 0.003	885	1002	1013
	> 0.001	2040	1347	2259
$\sigma \sin I$	> 0.01	6	7	9
	> 0.003	28	248	252
	> 0.001	300	642	650
	> 0.0003	1712	1101	2091
T_L	< 10000	499	478	490
	< 20000	892	777	789
	< 50000	1617	930	1603
	< 100000	2216	985	2220
	< 200000	2755	1014	2757
σe	< 0.0003	6687	129	6382
σ sin I	< 0.0001	7019	424	6856
$\sigma e \& \sigma \sin I$		5848	96	5625
$\sigma a \& \sigma e \& \sigma \sin I$		8009	307	7804